

## Detection of Cardiac Troponin I in Serum by CMK-3/AuNPs-based Electrochemical Sensor

Dan Chen<sup>1,#</sup>, Yong Gong<sup>2,#</sup>, Yinsheng Jin<sup>2,\*</sup>

<sup>1</sup> Department of Cardiovascular Medicine, Shiyan Renmin Hospital, Hubei University of Medicine, Hubei 442000, China

<sup>2</sup> Department of CCU, Shiyan Renmin Hospital, Hubei University of Medicine, Hubei 442000, China

#These two authors contributed equally

\*E-mail: [yinshengjinccu@163.com](mailto:yinshengjinccu@163.com)

Received: 25 February 2022 / Accepted: 4 April 2022 / Published: 6 June 2022

---

In this work, a novel signal amplification strategy was proposed based on nitrogen-doped ordered mesoporous carbon (CMK-3) and AuNPs nanocomposites (CMK-3/AuNPs). An immunosensor was fabricated to detect the concentration of cTnI in blood. CMK-3/AuNPs nanocomposites were used to modify the surface of gold electrode. The immunoreaction between the anti-cTnI and the target cTnI on the sensing interface can significantly reduce the electrocatalytic performance of H<sub>2</sub>O<sub>2</sub>, thus realizing the labeled free sensing analysis of cTnI. In the range of 10 fg/mL ~ 0.1 µg/mL, the catalytic current difference ( $\Delta I$ ) has a good linear relationship with the logarithm of cTnI concentration. The detection limit can be calculated to be 2.4 fg/mL (S/N=3). Based on the advantages of nanocomposites, the immunosensor has the advantages of low cost, fast response, high sensitivity, wide detection range and low detection limit. In addition, the immunosensor has good specificity and stability, which can be used to distinguish cTnI from other interfering substances.

---

**Keywords:** CMK-3; Catalase; Chronoamperometric response; Cardiac troponin I; Immunoreaction

### 1. INTRODUCTION

Cardiovascular diseases are the world's leading cause of death, accounting for about 31% of total deaths. Cardiovascular diseases include angina pectoris, acute myocardial infarction (AMI), unstable angina pectoris and heart failure. AMI in particular is considered to be the leading cause of death in patients with cardiovascular disease. The window period of thrombolysis and interventional therapy is 1-3 hours after the onset of AMI, which means that rapid diagnosis of AMI in early stage is the key to treatment. Traditional diagnosis of AMI mainly relies on angina symptom, electrocardiogram and biomarker detection. Biomarker detection is particularly important in the identification of patients with

atypical myocardial infarction. Among many biomarkers, cardiac troponin I (cTnI) is considered as an important indicator for early diagnosis of AMI [1–3]. It has high tissue specificity and clinical sensitivity, and can even reflect small areas of myocardial ischemia or necrosis [4]. When AMI occurs, serum cTnI levels are elevated within 12 h and remain elevated for 5 to 9 days. The concentration of cTnI in healthy people is usually less than 0.4 ng/mL, while the concentration higher than 2.0 ng/mL indicate an increased risk of serious cardiac events in the future [5,6].

At present, many methods have been used to detect the level of cTnI in blood samples, including enzyme-linked immunosorbent assay (ELISA), electrochemiluminescence immunoassay (ECL), chemiluminescence immunoassay and fluorescence immunoassay [7–11]. However, these methods have limitations such as long experimental period, complex experimental operation and low sensitivity. In this case, electrochemical immunosensor has attracted considerable attention because of its advantages of convenient operation, less sample consumption, fast response speed and low cost [12,13]. Although a lot of work has been done to improve the sensitivity of sensors in order to meet the needs of practical applications, methods of cTnI concentration detection by electrochemical sensors combined with nanomaterials have been reported in some literatures. However, the research in this area needs to be further explored [14–16]. Moreover, the synthesis of nanomaterials usually requires several steps or relatively harsh conditions, such as high temperature and high pressure. Therefore, in order to make up for the deficiency of existing studies, we proposed a new strategy to construct sandwich electrochemical immunosensor for cTnI detection [17,18].

Good electrical conductivity and large specific surface area contribute to improve the sensitivity of immunosensor. Ordered mesoporous carbon (CMK-3) is considered as a promising material because of its ordered two-dimensional hexagonal structure, highly active porous specific surface area, good electrical conductivity, thermal stability, simple operation and low manufacturing cost [19–22]. It has greatly expanded its applications in the fields of chemical catalysis, physical adsorption, chemical reactions, energy storage and biosensors [23]. In addition, gold nanoparticles (AuNPs) have good biocompatibility, excellent electronic conductivity, and provide sufficient binding sites for capturing antibody antibody (Ab1) in the presence of Au-NH<sub>2</sub> [24]. In addition, the negatively charged AuNPs can be absorbed onto the positively charged CMK-3 surface by electrostatic action [25,26]. Theoretically, CMK-3 and AuNPs can be immobilized on the surface of the electrode to improve the specific surface area and conductivity of the electrode, and increase the ability to capture the target material, thus effectively improving the sensitivity of the immunosensor. Based on the above analysis, this study proposed a simple, economical and sensitive electrochemical immunosensor for clinical detection of cTnI concentration in blood.

## 2. MATERIALS AND METHODS

Cardiac troponin I (cTnI), capture antibody (Ab1) and detection antibody (Ab2) were purchased from Shanghai Qiangyao Biotechnology Co., LTD. Chlorogold acid (HAuCl<sub>4</sub>·4H<sub>2</sub>O), bovine serum albumin (BSA) and chitosan (CS) were purchased from Sinopharm Chemical Reagents Co., LTD. Nitrogen-doped ordered mesoporous carbon (CMK-3) was purchased from Nanjing Pioneer Nano

Company. All of the other reagents were of analytical quality and were utilized without any additional purification or purifying steps.

CMK-3 was prepared by reference and were slightly modified during synthesis [27]. Firstly, 100 mg CS powder was dissolved in 20 mL 1% (V/V) acetic acid solution, and ultrasonic dispersion treatment was conducted for 1 h to obtain uniform pale-yellow colloid solution. Then the pH value of CS colloid solution was adjusted to 4.0 ~ 4.5 with 1 M NaOH. 1 mg CMK-3 was added to 1 mL CS solution and treated with ultrasound for 2 h until the color of the solution became uniform black without stratification. Finally, the black homogenous CMK-3 colloid solution was stored at 4°C for subsequent use.

The synthesis of gold nanoparticles (AuNPs, approx. 15 nm) was prepared by reducing HAuCl<sub>4</sub> with citrate according to previous literature. First, 100 mL 0.01% (w/v) HAuCl<sub>4</sub> solution was heated to boiling under continuous agitation for approximately 15 min. Then, 1 mL of 2% freshly prepared trisodium citrate solution was added to the above solution drop by drop. Then, continue stirring for another 15 min and observe that the color of the solution changes from light yellow to wine red. This means the formation of AuNPs. Finally, the AuNPs colloidal solution was cooled to room temperature and stored at 4°C in a brown flask (to avoid light-induced aggregation) for subsequent use.

Polish the gold electrode (GE) with 0.3 and 0.05 μm alumina slurry for at least 3 min. Then, the impurities on the surface of the GE were removed by continuous ultrasonic treatment in water, anhydrous ethanol for 3 min. The GE was then immersed in a freshly prepared piranha solution (98% H<sub>2</sub>SO<sub>4</sub>:30% H<sub>2</sub>O<sub>2</sub>, 3:1 v) for 5 min and thoroughly rinsed with ultrapure water. 5 μL CMK-3 (1 mg mL<sup>-1</sup>) were added to the polished GE surface and dried at room temperature for 4 h (CMK-3/GE). Then 5 μL AuNPs colloidal solution was dropped onto the surface of the modified electrode and dried at room temperature for 2 h (AuNPs/CMK-3/GE). AuNPs/CMK-3/GE modified electrode (Anti-cTnI/AuNPs/CMK-3/GE) was prepared by dropping 10 μL immunohistochemical PBS solution containing 4 μg/mL anti-cTnI onto the AuNPs/CMK-3/GE surface and placing it at 4 °C for 3 h. The modified electrode was incubated in 200 μL 1% BSA solution for 2 h, the remaining active sites on AuNPs/CMK-3 were closed. The surface of the electrode was washed with water to prepare a cTnI electrochemical sensor.

The cTnI electrochemical sensor was immersed in 0.1 M PBS (pH 7.4) with different concentrations of cTnI and reacted at room temperature for 50 min. The sensor was removed and rinsed with 0.1 M PBS. Chronoamperometric response was performed in 0.1 M PBS (pH 7.0) containing 5 mM H<sub>2</sub>O<sub>2</sub>, with electric potential of -0.5 V. 0.5 mM [Fe(CN)<sub>6</sub>]<sup>3-/4-</sup> + 0.5 M KCl was used as probe, and cyclic voltammetry (CV) and electrochemical impedance (EIS) were used to characterize the electrode. CV potential scanning range is -0.2 V to + 0.6 V, the scanning rate is 0.1 V/s. The EIS frequency range is 1 ~ 10<sup>5</sup> Hz, and the test voltage is 0.211 V.

### 3. RESULTS AND DISCUSSION

The morphology of CMK-3 was studied by scanning electron microscope (SEM). As shown in Figure 1A, CMK-3 presents nanorods formed by the gathered rod like matter. The surface is rough and porous with good pore size and large pore volume, which can provide a large specific surface area and

improve the sensitivity of the sensor [28]. UV-vis was also used to characterize AuNPs synthesis. In Figure 1B, an obvious absorption peak was observed at 525 nm, further indicating the successful synthesis of AuNPs.

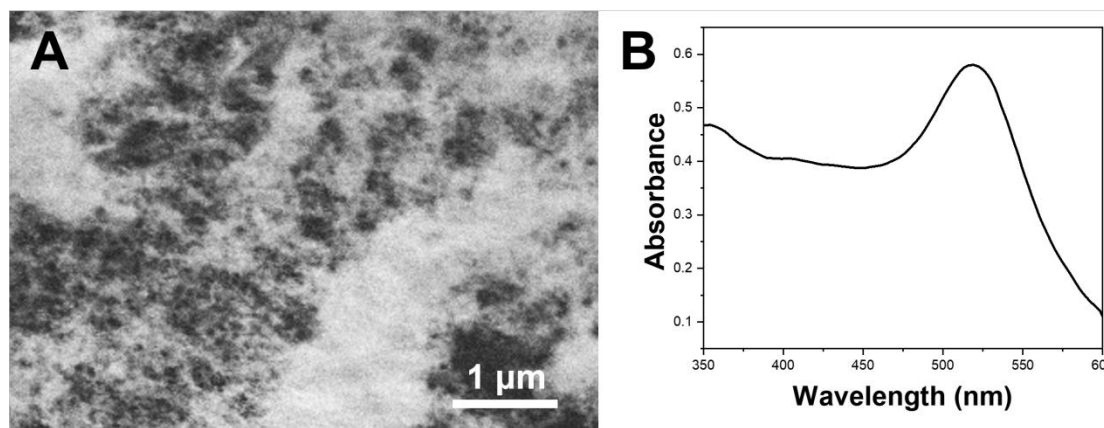


**Figure 1.** (A) SEM and (B) UV-vis spectrum of AuNPs/CMK-3.

We verified the electrode modification by using CV in PBS containing 5 mM  $K_3Fe(CN)_6/K_4Fe(CN)_6$  and 0.1M KCl. As shown in Figure 2A, bare GE shows a good reversible redox peak, which is attributed to the redox of  $[Fe(CN)_6]^{3-/4-}$ , proving that the polished bare GE has good electrical conductivity. The obvious increase of current response after CMK-3 deposition on GE is due to the increase of effective pore specific surface area and good electrical conductivity of CMK-3 [29]. Then, the highest redox peak was obtained by modifying AuNPs on the CMK-3/GE surface, because the excellent conductivity of AuNPs can significantly promote the electron transfer process on the modified electrode. After Ab1 was incubated on the modified electrode, the redox peak current begins to decrease because the bioactive substance blocks the electron transfer efficiency. This proves that Ab1 is successfully fixed to the AuNPs/CMK-3/GE surface via the Au-NH<sub>2</sub> bond [30]. Subsequently, the redox peak decreased again after the non-specific sites were blocked by the introduction of non-electroactive substance BSA on the electrode surface [31]. After cTnI incubation with BSA/Ab1/AuNPs/CMK-3/GE, the redox peak was further reduced, indicating the specific recognition and binding between Ab1 and cTnI.

In addition, electrical impedance spectroscopy (EIS) was used to verify the successful modification of the electrode surface (Figure 2B). The diameter of the semicircle is proportional to the charge transfer resistance ( $R_{et}$ ) [32]. The small  $R_{et}$  of bare GE indicates that GE has good conductivity. When AuNPs and CMK-3 deposited successively on GE surface, the semicircle diameter decreased [33]. This indicates that AuNPs and CMK-3 can accelerate electron transfer. However, when Ab1 was immobilized on the modified electrode and BSA was added to block the remaining active site, the semicircle diameter increased significantly due to non-conductive materials blocking electron transfer, which was consistent with CV results. Moreover, in the presence of cTnI [34],  $R_{et}$  increases to a maximum. This is consistent with the fact that protein hydrophobic layers isolate conducting carriers

[35]. In summary, the CV and EIS results mutually confirm the success of the layered electrode assembly.

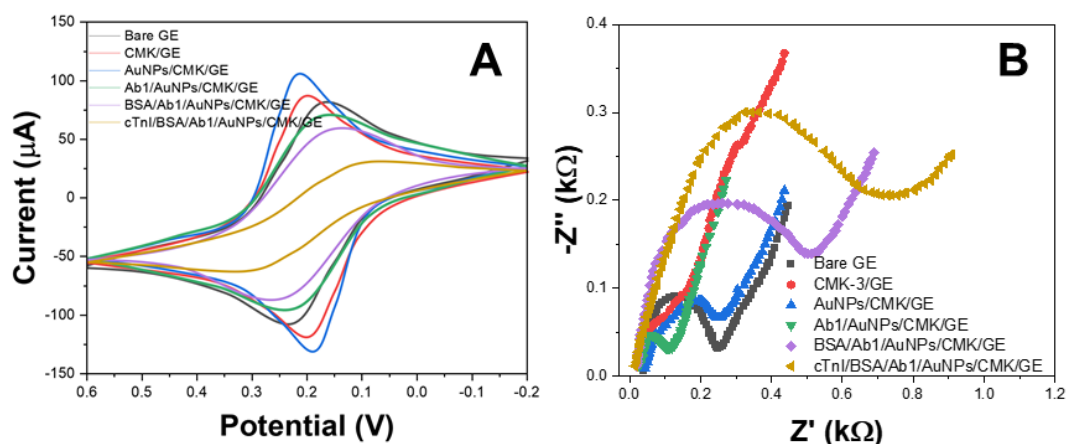


**Figure 2.** (A) CV and (B) EIS of bare GE, CMK-3/GE, AuNPs/CMK-3/GE, Ab1/AuNPs/CMK-3/GE, BSA/Ab1/AuNPs/CMK-3/GE and cTnI/BSA/Ab1/AuNPs/CMK-3/GE in 0.1 M PBS containing 5 mM  $[\text{Fe}(\text{CN})_6]^{3-/4-}$  + 0.1 M KCl.

The electrocatalytic performance of composite sensor material AuNPs/CMK-3 and the influence of anti-cTnI immobilization on its catalytic performance were investigated by timing amperometry [36,37]. The results are shown in Figure 3. The AuNPs/CMK-3 modified electrode has very low background current in 0.1 M PBS (pH 7.0) blank solution without  $\text{H}_2\text{O}_2$ . When  $\text{H}_2\text{O}_2$  was added into PBS solution, the steady-state catalytic current increased significantly, indicating that AuNPs/CMK-3 had catalase mimetic catalytic activity [38,39]. CMK-3 and AuNPs modified electrodes were prepared and their catalytic activity to  $\text{H}_2\text{O}_2$  was investigated. The results showed that no significant catalytic current was observed for  $\text{H}_2\text{O}_2$  on CMK-3 modified electrode, indicating that CMK-3 did not mimic enzyme activity [40]. The steady-state current of  $\text{H}_2\text{O}_2$  AuNPs modified electrode increased obviously, indicating that the simulated enzyme catalytic activity of AuNPs/CMK-3 composite mainly came from AuNPs. At the same time, the steady-state catalytic current value of the single AuNPs modified electrode is smaller than that of the composite electrode, indicating that the high conductivity of CMK-3 contributes to the enhancement of the AuNPs/CMK-3 catalytic current [41–43]. When AuNPs/CMK-3 modified electrode was immobilized on the surface of anti-cTnI, the steady state catalytic current decreased [44,45]. This indicates that immobilization of anti-cTnI inhibits AuNPs/CMK-3 electrocatalysis.

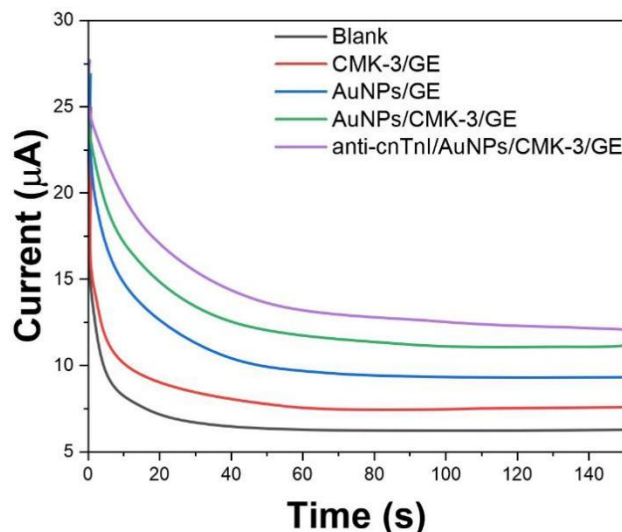


**Figure 3.** Chronoamperometric response of AuNPs/CMK-3/GE in blank solution (0.1 M PBS buffer, pH = 7.0), and CMK-3/GE, AuNPs/GE, AuNPs/CMK-3/GE, anti-cTnI/AuNPs/CMK-3/GE in 0.1 M PBS solution (pH = 7.0) with 5 mM H<sub>2</sub>O<sub>2</sub>. Applied potential: -0.6 V.

We then optimized the amount of AuNPs/CMK-3, anti-cTnI immobilization time and the time of sensor and cTnI immunity. After casting of AuNPs/CMK-3 dispersions (1 mg/mL) of GE surface, the relationship curve between  $R_{et}$  and AuNPs/CMK-3 modification measured in  $[\text{Fe}(\text{CN})_6]^{3-/4-}$  is shown in Figure 4A. As the volume of AuNPs/CMK-3 increases,  $R_{et}$  decreases gradually. When the volume reaches 10  $\mu\text{L}$ ,  $R_{et}$  reaches stability. This indicates that AuNPs/CMK-3 has the maximum promoting ability for electron transfer of electroactive substances on the electrode surface [46]. Therefore, the optimal modification amount of 4 mg/mL AuNPs/CMK-3 dispersion was determined to be 10  $\mu\text{L}$ .

Subsequently, the activated AuNPs/CMK-3/GE was immersed in 4  $\mu\text{g/mL}$  anti-cTnI solution for antibody immobilization reaction, and the effect of anti-cTnI immobilization time on the electrochemical impedance of the electrode was investigated [47]. The results show that the  $R_{et}$  increases with the extension of T1. When T1 reached 3 h,  $R_{et}$  reached its maximum value and remained stable (Figure 4B). This indicates that the immobilization of anti-cTnI on AuNPs/CMK-3/GE surface is saturated. Therefore, the immobilization time for selecting anti-cTnI is 3 h.

The influence of the time of immune reaction of cTnI and antibody on the sensor surface is shown in Figure 4C. The  $R_{et}$  gradually increases with the extension of time, which indicating that the antigen-antibody complex formed by the immune reaction on the electrode surface is increasing. When the time reached 50 min,  $R_{et}$  did not increase significantly, indicating that the immune reaction between anti-CTNI and cTnI on the electrode surface was balanced [48]. Therefore, the action time of cTnI was selected to be 50 min.

The catalytic reduction performance of H<sub>2</sub>O<sub>2</sub> at different application potentials ( $E_a$ ) was investigated by timing amperometry. The results show that when  $E_a$  decreases from -0.3 V to -0.6 V, the steady-state catalytic current increases and then becomes stable. Therefore, the applied potential for timing amperometric analysis was -0.6 V.

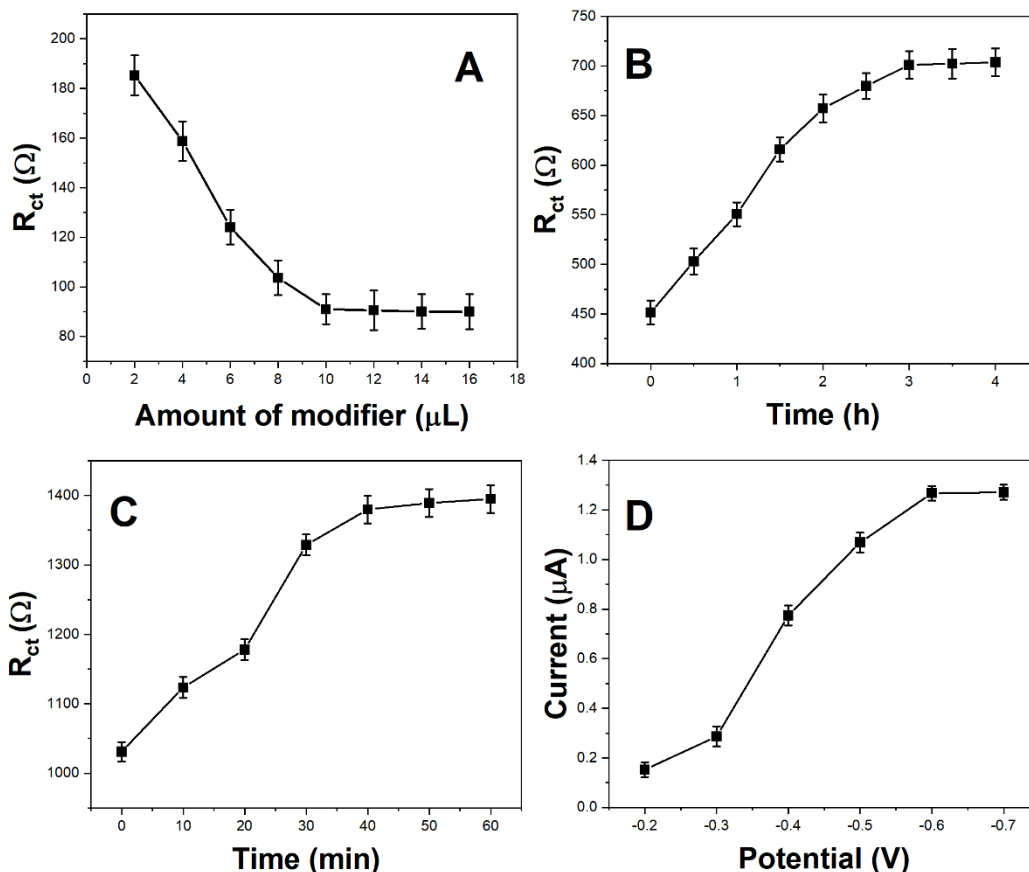


**Figure 4.** Effects of (A) amount of AuNPs/CMK-3 dispersion, (B) immobilization time of anti-cTnI, (C) immune reaction time on the values of  $R_{ct}$  of electrodes. (D) Relationship between catalytic currents and applied potentials.

Under the optimal experimental conditions, the prepared sensors were exposed to different concentrations of cTnI for immune response, and then timed amperometric test was performed in PBS solution containing 5 mM  $\text{H}_2\text{O}_2$  (0.1 M, pH 7.0). As shown in Figure 5A, the steady-state catalytic current gradually decreases with the increase of the concentration of target molecule cTnI. This indicates that anti-cTnI binds specifically with cTnI on the sensor surface, and the complex formed gradually increases. The effect of AuNPs/CMK-3 on  $\text{H}_2\text{O}_2$  oxidation was enhanced. When cTnI concentration is in the range of 10 fg/mL  $\sim$  0.1  $\mu\text{g}/\text{mL}$ , the steady-state catalytic current difference ( $\Delta I$ ) after immune reaction has a good linear relationship with the negative logarithm of cTnI concentration (Figure 5B). The detection limit can be calculated as 2.4 fg/mL ( $S/N=3$ ). Compared with cTnI electrochemical sensors reported in the literature, this sensor has higher sensitivity and wider detection range (Table 1). This is due to the AuNPs are directly immobilization on the electrode surface in this study, which can achieve catalytic signal amplification more effectively than traditional bio-probe labeling. CMK-3 with high specific surface area and high conductivity further enhances the catalytic current. The change of the microenvironment of the sensing interface caused by immune reaction can lead to the change of the catalytic activity of CMK-3, thus improving the sensitivity of the sensor.

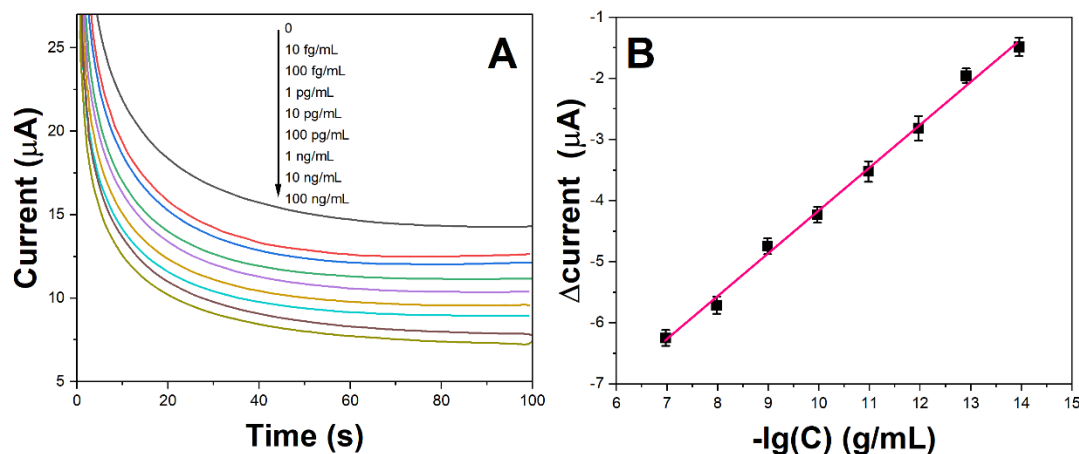


**Figure 5.** (A) Chronoamperometric response of anti-cTnI/AuNPs/CMK-3/GE in 0.1 M PBS containing 5 mM H<sub>2</sub>O<sub>2</sub> with 0, 10 fg/mL, 100 fg/mL, 1 pg/mL, 10 pg/mL, 100 pg/mL, 1 ng/mL, 10 ng/mL and 100 ng/mL of cTnI. (B) Plot of  $\Delta I$  versus  $-\lg C_{cTnI}$

**Table 1.** Comparison of analytical performance of the anti-cTnI/AuNPs/CMK-3/GE with other reported cTnI biosensors.

Sensor	Linear detection range	LOD	Reference
Immune probe-assisted SPR biosensor	-	3.75 ng/mL	[49]
Colorimetric sensing	-	0.2 ng/mL	[50]
Electrochemical aptasensor	1~10 000 pM	1.0 pM	[51]
Electrochemical immunosensor	10~100 pg/mL	1.9 pg/mL	[52]
anti-cTnI/AuNPs/CMK-3/GE	10 fg /mL~0.1 µg /mL	2.4 fg /mL	This work

Hb is a common biological molecule in blood, and its content is related to polycythemia vera, various anemia, leukemia and other diseases. Myoglobin (Myo) is a small pigment protein that can transport and store oxygen in muscle cells. When heart muscle is damaged, Myo also diffuses out of heart muscle cells and into the bloodstream. In this study, the specificity of the sensor for cTnI detection was investigated using two potential interferers, Hb and Myo, as control molecules. When the concentration of Hb, Myo and cTnI was 0.1 µg/mL, the signal of Hb and Myo solution was close to that of blank solution. This indicates that the sensor does not respond to Hb and Myo. However, the signal of cTnI and the mixed liquid is significantly less than that of blank liquid, and the two signals are basically consistent, indicating that the sensor has a good specificity for cTnI.



We investigated the reproducibility of anti- cTnI/AuNPs/CMK-3/GE. We prepared 10 sensors in parallel and determined 0.2  $\mu\text{g/mL}$  cTnI solution. The relative standard deviation (RSD) of the analysis signal ( $\Delta I$ ) is 3.6%, indicating that the sensor has good reproducibility. The anti-cTnI/AuNPs/CMK-3/GE was stored at 4  $^{\circ}\text{C}$  for 10 days and the time-amperometric response signal was measured in blank solution every 2 days. After 10 days, the signal attenuated to 93.4% of the original signal. On the 10th day, the sensor was used to detect 0.2  $\mu\text{g/mL}$  cTnI solution, and the measured concentration was 0.21  $\mu\text{g/mL}$ , indicating that the sensor has good stability.

We added different amounts of cTnI standard solution into blank serum samples and used this sensor for detection (Table 2). The relative standard deviations (RSD) at 20  $\text{pg/mL}$ , 1.00  $\text{ng/mL}$  and 50  $\text{ng/mL}$  were 3.6%, 4.2% and 5.1%, respectively. Their recoveries were 97.4%, 101.3% and 104.1%, respectively, indicating that the sensor can be used for cTnI analysis in actual serum samples.

**Table 2.** Detection of cTnI in serum samples (n=3)

Sample	Addition	Found	Recovery	RSD
1	20 $\text{pg/mL}$	19.48 $\text{pg/mL}$	97.4%	3.60 %
2	1.00 $\text{ng/mL}$	1.02 $\text{ng/mL}$	102.0%	4.20 %
3	50 $\text{ng/mL}$	52.05 $\text{ng/mL}$	104.1%	5.10 %

#### 4. CONCLUSION

In this work, AuNPs/CMK-3 was synthesized and a novel cTnI labeled free electrochemical immunosensor was constructed. Based on the high conductivity of CMK-3, the catalase activity of AuNPs and the inhibitory effect of antigen antibody immune reaction on the catalytic activity of mimics, the sensor showed excellent performance for cTnI analysis. Under the optimal conditions, the linear range of cTnI detection by the sensor is 10  $\text{fg/mL}$  ~ 0.1  $\mu\text{g/mL}$ , and the detection limit is 2.4  $\text{fg/mL}$ . This sensor can recognize cTnI with high specificity, and can be used for accurate analysis of cTnI in human serum samples, providing a new technical reference for clinical detection of markers of myocardial injury.

#### References

1. S. Natarajan, J. Jayaraj, D.M.F. Prazeres, *Biosensors*, 11 (2021) 49.
2. L. Miao, L. Jiao, Q. Tang, H. Li, L. Zhang, Q. Wei, *Sens. Actuators B Chem.*, 288 (2019) 60.
3. J. Li, S. Zhang, L. Zhang, Y. Zhang, H. Zhang, C. Zhang, X. Xuan, M. Wang, J. Zhang, Y. Yuan, *Front. Chem.*, 9 (2021) 7.
4. K. Phonklam, R. Wannapob, W. Sriwimol, P. Thavarungkul, T. Phairatana, *Sens. Actuators B Chem.*, 308 (2020) 127630.
5. N. Qvit, A.J. Lin, A. Elezaby, N.P. Ostberg, J.C. Campos, J.C. Ferreira, D. Mochly-Rosen, *Pharmaceuticals*, 15 (2022) 271.
6. A.R. Oh, J. Park, S. Lee, K. Yang, J.-H. Choi, K. Kim, J. Ahn, J.D. Sung, S.-H. Lee, *Diagnostics*, 11 (2021) 2229.
7. D. Çimen, N. Bereli, S. Günaydın, A. Denizli, *Talanta*, 219 (2020) 121259.

8. T.-H. Lee, L.-C. Chen, E. Wang, C.-C. Wang, Y.-R. Lin, W.-L. Chen, *Biosensors*, 11 (2021) 210.
9. P.A. Kavsak, M.K. Hewitt, S.E. Mondoux, J.O. Cerasuolo, J. Ma, N. Clayton, M. McQueen, L.E. Griffith, R. Perez, H. Seow, *J. Cardiovasc. Dev. Dis.*, 8 (2021) 97.
10. D. Sun, X. Lin, J. Lu, P. Wei, Z. Luo, X. Lu, Z. Chen, L. Zhang, *Biosens. Bioelectron.*, 142 (2019) 111578.
11. J. Zhang, T. LakshmiPriya, S.C. Gopinath, *ACS Omega*, 5 (2020) 25899.
12. Y. Han, X. Su, L. Fan, Z. Liu, Y. Guo, *Microchem. J.*, 169 (2021) 106598.
13. D. Sun, Z. Luo, J. Lu, S. Zhang, T. Che, Z. Chen, L. Zhang, *Biosens. Bioelectron.*, 134 (2019) 49.
14. H. Zhao, X. Du, H. Dong, D. Jin, F. Tang, Q. Liu, P. Wang, L. Chen, P. Zhao, Y. Li, *Biosens. Bioelectron.*, 175 (2021) 112883.
15. Z. Mokhtari, H. Khajehsharifi, S. Hashemnia, Z. Solati, R. Azimpanah, S. Shahrokhian, *Sens. Actuators B Chem.*, 320 (2020) 128316.
16. J. de F. Giarola, D.E. Souto, L.T. Kubota, *Anal. Sci.*, 37 (2021) 1007–1013.
17. X. Qian, X. Zhou, X. Ran, H. Ni, Z. Li, Q. Qu, J. Li, G. Du, L. Yang, *Biosens. Bioelectron.*, 130 (2019) 214.
18. V.T. Tran, H. Ju, *Biomedicines*, 9 (2021) 448.
19. R. Radha, S.K. Shahzadi, M.H. Al-Sayah, *Molecules*, 26 (2021) 4812.
20. G.-R. Han, M.-G. Kim, *Sensors*, 20 (2020) 2593.
21. O. Krupin, P. Berini, *Sensors*, 19 (2019) 631.
22. N. Ma, T. Zhang, T. Yan, X. Kuang, H. Wang, D. Wu, Q. Wei, *Biosens. Bioelectron.*, 143 (2019) 111608.
23. Y. Wang, Y. Yang, C. Chen, S. Wang, H. Wang, W. Jing, N. Tao, *ACS Sens.*, 5 (2020) 1126.
24. P. Gopinathan, A. Sinha, Y.-D. Chung, S.-C. Shiesh, G.-B. Lee, *Analyst*, 144 (2019) 4943.
25. S. Vasantham, R. Alhans, C. Singhal, S. Nagabooshanam, S. Nissar, T. Basu, S.C. Ray, S. Wadhwa, J. Narang, A. Mathur, *Biomed. Microdevices*, 22 (2020) 1.
26. W. Dong, X. Mo, Y. Wang, Q. Lei, H. Li, *Anal. Lett.*, 53 (2020) 1888.
27. S.A. Kitte, T. Tafese, C. Xu, M. Saqib, H. Li, Y. Jin, *Talanta*, 221 (2021) 121674.
28. J. Luo, S. Li, M. Xu, M. Guan, M. Yang, J. Ren, Y. Zhang, Y. Zeng, *AIP Adv.*, 10 (2020) 115205.
29. K. Dhara, D.R. Mahapatra, *Microchem. J.*, 156 (2020) 104857.
30. D. Magrì, V. Mastromarino, G. Gallo, E. Zachara, F. Re, P. Agostoni, D. Giordano, S. Rubattu, M. Forte, M. Cotugno, *J. Clin. Med.*, 9 (2020) 1636.
31. M. Wu, X. Zhang, R. Wu, G. Wang, J. Li, Y. Chai, H. Shen, L.S. Li, *Anal. Lett.*, 53 (2020) 1757.
32. Y. Chen, L.-P. Mei, J.-J. Feng, P.-X. Yuan, X. Luo, A.-J. Wang, *Biosens. Bioelectron.*, 145 (2019) 111638.
33. H. Lee, H. Youn, A. Hwang, H. Lee, J.Y. Park, W. Kim, Y. Yoo, C. Ban, T. Kang, B. Kim, *Nanomaterials*, 10 (2020) 1402.
34. M. Yan, J. Ye, Q. Zhu, L. Zhu, J. Huang, X. Yang, *Anal. Chem.*, 91 (2019) 10156.
35. A. Pourali, M.R. Rashidi, J. Barar, G. Pavon-Djavid, Y. Omid, *TrAC Trends Anal. Chem.*, 134 (2021) 116123.
36. D. Fan, X. Liu, X. Shao, Y. Zhang, N. Zhang, X. Wang, Q. Wei, H. Ju, *Microchim. Acta*, 187 (2020) 1.
37. M. Negahdary, M. Behjati-Ardakani, H. Heli, N. Sattarahmady, *Int. J. Mol. Cell. Med.*, 8 (2019) 271.
38. N.F.N. Azam, N.A. Mohammad, S.A. Lim, M.U. Ahmed, *Anal. Sci.* (2019) 19P105.
39. J. Zhao, J. Du, J. Luo, S. Chen, R. Yuan, *Sens. Actuators B Chem.*, 311 (2020) 127934.
40. B. Demirbakan, M.K. Sezgintürk, *Talanta*, 213 (2020) 120779.

41. Y. Takahashi, M. Satoh, H. Ohmomo, F. Tanaka, T. Osaki, K. Tanno, T. Nasu, K. Sakata, Y. Morino, K. Sobue, *Biomarkers*, 24 (2019) 566.
42. C. Bao, X. Liu, X. Shao, X. Ren, Y. Zhang, X. Sun, D. Fan, Q. Wei, H. Ju, *Biosens. Bioelectron.*, 157 (2020) 112157.
43. Z. Luo, D. Sun, Y. Tong, Y. Zhong, Z. Chen, *Microchim. Acta*, 186 (2019) 1–10.
44. T. Lee, Y. Lee, S.Y. Park, K. Hong, Y. Kim, C. Park, Y.-H. Chung, M.-H. Lee, J. Min, *Colloids Surf. B Biointerfaces*, 175 (2019) 343.
45. T. Lee, J. Kim, I. Nam, Y. Lee, H.E. Kim, H. Sohn, S.-E. Kim, J. Yoon, S.W. Seo, M.-H. Lee, *Nanomaterials*, 9 (2019) 1000.
46. G. Fitzgerald, R. Kerley, T.J. Kiernan, *Expert Rev. Cardiovasc. Ther.*, 17 (2019) 763–770.
47. X. Wang, X. Wang, Y. Han, H. Li, Q. Kang, P. Wang, F. Zhou, *ACS Appl. Nano Mater.*, 2 (2019) 7170.
48. X. Zhang, H. Lv, Y. Li, C. Zhang, P. Wang, Q. Liu, B. Ai, Z. Xu, Z. Zhao, *J. Mater. Chem. B*, 7 (2019) 1460.
49. F. Chen, Q. Wu, D. Song, X. Wang, P. Ma, Y. Sun, *Colloids Surf. B Biointerfaces*, 177 (2019) 105.
50. X. Liu, Y. Wang, P. Chen, A. McCadden, A. Palaniappan, J. Zhang, B. Liedberg, *Acs Sens.*, 1 (2016) 1416.
51. H. Jo, H. Gu, W. Jeon, H. Youn, J. Her, S.-K. Kim, J. Lee, J.H. Shin, C. Ban, *Anal. Chem.*, 87 (2015) 9869.
52. S. Dhawan, S. Sadanandan, V. Haridas, N.H. Voelcker, B. Prieto-Simón, *Biosens. Bioelectron.*, 99 (2018) 486.